Mechanism of controlling turbulent channel flow with the effect of spanwise Lorentz force distribution*

Yang Han(韩洋), Hui Zhang(张辉)†, Bao-Chun Fan(范宝春),
Jian Li(李健), Dai-Wen Jiang(江代文), and Zi-Jie Zhao(赵子杰)

Science and Technology on Transient Physics Laboratory, Nanjing University of Science and Technology, Nanjing 210094, *China*

(Received 24 March 2017; revised manuscript received 13 April 2017; published online 10 July 2017)

A direct numerical simulation (DNS) is performed to investigate the control effect and mechanism of turbulent channel flow with the distribution of spanwise Lorentz force. A sinusoidal distribution of constant spanwise Lorentz force is selected, of which the control effects, such as flow characters, mean Reynolds stress, and drag reductions, at different parameters of amplitude A and wave number k_x are discussed. The results indicate that the control effects vary with the parameter A and k_x. With the increase of A, the drag reduction rate D_r first increases and then decreases rapidly at low k_x, and slowly at high k_x. The low drag reduction (or even drag increase) is due to a weak suppression or even the enhancements of the random velocity fluctuation and mean Reynolds stress. The efficient drag reduction is due to the quasi-streamwise vortex structure induced by Lorentz force, which contributes to suppressing the random velocity fluctuation and mean Reynolds stress, and the negative vorticity improves the distribution of streamwise velocity. Therefore, the optimal control effect with a drag reduction of up to 58% can be obtained.

Keywords: flow control, turbulent channel flow, Lorentz force, direct numerical simulation

PACS: 47.85.L–, 47.85.lb **DOI:** 10.1088/1674-1056/26/8/084704

1. Introduction

The boundary layer generated on surface of transport vehicle by viscous fluid will cause deceleration, vibration and unstability.[1–5] Moreover, turbulent boundary layer can increase the skin-friction drag rapidly. With the recent development of turbulence theories, the characters and essences of turbulent coherent structures have been understood in depth. Many strategies and approaches of control and drag reduction based on turbulence theories have been studied so far,resulting in substantial progress. These technologies can be widely used for improving kinetic stability, propelling efficiency and reducing energy consumption.

The technologies of flow control can be divided into passive approaches without energy input, and active approaches with energy input.[6–11] One of active control approaches is based on changing the near-wall flow by introducing transverse motion including a spanwise motion combined with a wall-normal deflection and a spanwise in-plane motion parallel to the wall.[12] One form of transverse in-plane motion is a spanwise oscillating excitation via body force including plasma in air[13] and Lorentz force in weakly conductive fluid.The numerical investigations focused on turbulence control by spanwise oscillating Lorentz force[14,15] were conducted with remarkable drag reductions and significant suppression on near-wall coherent structure obtained at optimal parameters. The tilted streaks and quasi-streamwise vortex structure were observed near the wall in the above investigations. Experiments with elaborately designed electromagnetic devices[16–18] confirmed the above control effects and provided some application approaches. Another approach is to introduce the transverse in-plane motion induced by a travelling wave excitation via spanwise Lorentz force. Investigations based on direct numerical simulation (DNS) were performed, resulting in efficient control effects of drag reduction and suppression on turbulence, while the phenomena of the modification to the near-wall flow are different. Two kinds of typical vortex structures induced by spanwise wave and streamwise wave excitations were observed and regarded as main factors of the suppressing streaks and streamwise vortex structures. Du and Karniadakis,[19] and Du *et al.*[20] performed a DNS and investigated wall-bounded flow controlled by a spanwise travelling wave induced by a spanwise Lorentz force. They analyzed the near-wall turbulent structure, flow character together with Reynolds stress and obtained a drag reduction of up to 30%. Xu and Choi[21] experimentally confirmed a drag reduction of 28.9% and a drag increase of 22.8%, respectively.[21] They also observed the spanwise displacements of the streak structure, which play an important role in the process of the drag reduction by spanwise travelling wave actuation. For streamwise waves, Quadrio,[11] Quadrio and Ricco,[22] and Viotti and Quadrio[23] studied the streamwise travelling and standing waves of velocity imposed at the walls of a plane turbulent channel flow by DNS and obtained a drag

*Project supported by the National Natural Science Foundation of China (Grant Nos. 11672135 and 11202102), the Fundamental Research Funds for the Central Universities, China (Grant No. 30916011347), and a Foundation for the Author of National Excellent Doctoral Dissertation, China (Grant No. 201461).

†Corresponding author. E-mail: zhanghui1902@hotmail.com

© 2017 Chinese Physical Society and IOP Publishing Ltd

reduction up to 48% for travelling waves and 52% for standing waves. Yin *et al.*[24] presented a detached eddy simulation to analyze the characteristics for the flow around a circular cylinder with a turbulent boundary layer. Our research group[25–27] investigated the control and drag reduction effects numerically in a channel flow via a streamwise travelling wave and a spacial oscillation (a streamwise standing wave) induced by spanwise Lorentz force. The results showed that the turbulent bursts which mainly contributed to the turbulent skin-friction drag varied with wave number k_x, and that the drag reduction could be optimized with k_x and was affected by the oscillation parameters.

The above research results indicated that the efficient turbulence control can be obtained with the oscillating and traveling wave motions induced by Lorentz force. However, the Lorentz force almost varies with time. Therefore, the character of the steady flow field under control, corresponding to the distribution of the force, cannot be obtained, nor can the potential relations among the Lorentz force distribution, flow structures and drag reduction. Therefore, additional in-depth investigations are necessary.

In this paper, a direct numerical simulation based on the Fourier–Chebyshev spectral method is performed to investigate the control of turbulence via a spanwise sinusoidal steady Lorentz force. The characters of flow fields, distributions of Reynolds shear stress and drag reductions at different parameters of amplitude and streamwise wave number are compared and discussed. Then, the typical structures and their effects are described to reveal the potential relation among the distribution of Lorentz force, flow structures, Reynolds shear stress and drag reduction.

2. Numerical scheme

2.1. Governing equation

The problem is to control a fully developed turbulent flow in a weakly conductive fluid in a channel covered with electromagnetic actuators only on the lower wall. The flow is governed by the incompressible Navier-Stokes equations with externally imposed body force term written as

$$\frac{\partial \boldsymbol{u}}{\partial t} + \boldsymbol{u}\cdot\nabla\boldsymbol{u} = -\nabla p + \nu\nabla^2\boldsymbol{u} + \boldsymbol{f}, \tag{1}$$

$$\nabla\cdot\boldsymbol{u} = 0. \tag{2}$$

Here, all variables are nondimensionalized with respect to the channel half width h and the center line velocity U_c. $\boldsymbol{u}$ is the velocity vector, p the pressure, ν the kinematic viscosity, and $\boldsymbol{f}$ the Lorentz force given by

$$\boldsymbol{f} = (0, 0, f_z), \tag{3}$$

where

$$f_z = A\,\mathrm{e}^{-y/\Delta}\sin\left(\frac{2\pi}{L_x}k_x x\right). \tag{4}$$

Here, f_z is spanwise Lorentz force with the sinusoidal distributions along the streamwise direction, which is independent of time. Moreover, A is the dimensionless amplitude of excitation, $\Delta = 0.02$ is the effective penetration of the Lorentz force, and $k_x = L_x/\lambda_x$ is the streamwise wave number, where λ_x is the streamwise wave length and L_x is the streamwise channel length.

The numerical method adopted here is based on the standard Fourier–Chebyshev spectral method. In the homogeneous directions, streamwise and spanwise directions, a dealiased Fourier method is used for the spatial derivatives, and the periodic conditions are applied. Then a Chebyshev-tau method is used in the wall normal direction, and the usual no-slip and no-penetration conditions are applied to the wall. The time advancement is carried out by using a semi-implicit back-differentiation formula method with the third-order accuracy. To ensure that the computed solutions satisfy both the incompressibility constraint and the momentum equation, a Chebyshev-τ influence-matrix method is employed for the linear term and the pressure term. Aliasing errors in the streamwise and spanwise directions are removed by spectral truncation method referred to as 3/2-rule.

The size of the computational domain, which is shown in Fig. 1, is $4\pi/3 \times 2 \times 2\pi/3$ (approximately $754 \times 360 \times 377$ wall units) corresponding to the streamwise, normal and spanwise directions, respectively. The uniform grid spacing is used in the streamwise and spanwise directions. However, in the normal direction, the minimum spacing in the near-wall region and the maximum spacing at the channel center line are $\Delta y^+ = 0.2(\sim 6\times10^{-2}\eta)$ and $\Delta y^+ = 8.6(\sim 2.4\eta)$, respectively, where superscript "+" refers to the quantity in wall units and η is the Kolmogorov length scale. The longitudinal flow rate is kept constant during the simulation, and the corresponding Reynolds number is $Re = 4000$ based on channel half width h and the center line velocity U_c.

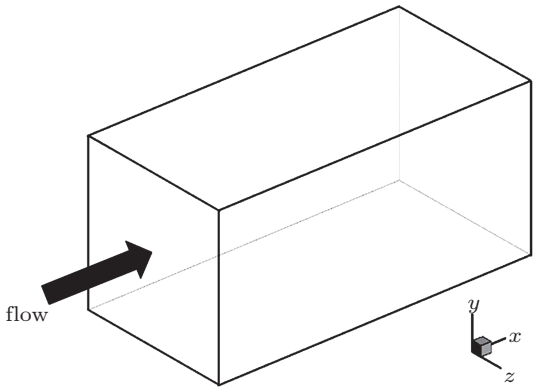


Fig. 1. Schematic diagram of computational domain.

2.2. Program verification

To test the algorithm and code, an uncontrolled turbulent flow field at $Re = 4000$ is calculated to compare with the results obtained by Kim *et al.*[28] As shown in Fig. 2, the mean velocity profiles in this paper accord with those in Ref. [28] and the classic wall law.

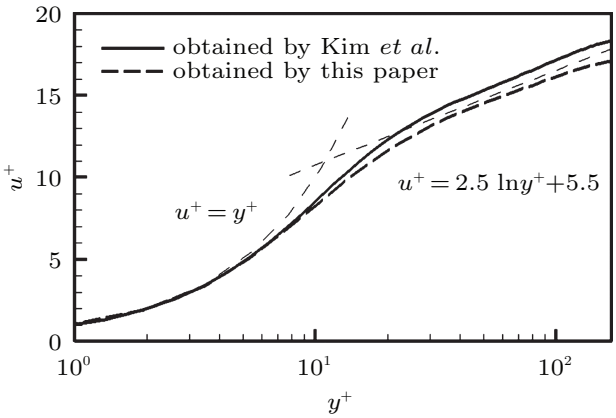


Fig. 2. Logarithmic profiles of mean velocity.

3. Results and discussion

3.1. Induced flow fields

The spanwise Lorentz force defined by Eq. (4) is independent of time or flow, of which the distribution is shown in Fig. 3. When this force is introduced into a static flow field, a spanwise motion is induced and shear layers with streamwise vorticities are generated in the near-wall region, which are known as Stokes layers. The distribution of induced spanwise velocity in a controlled laminar flow, $Re = 4000$ for example, is shown in Fig. 4, where the red and blue areas refer to the positive and negative spanwise velocity, respectively. Due to the main flow, the distribution of the spanwise velocity is inclined, and it is asymmetric, but still periodical, resulting in the periodical shear layers of spanwise velocity and alternately positive and negative streamwise vorticities.

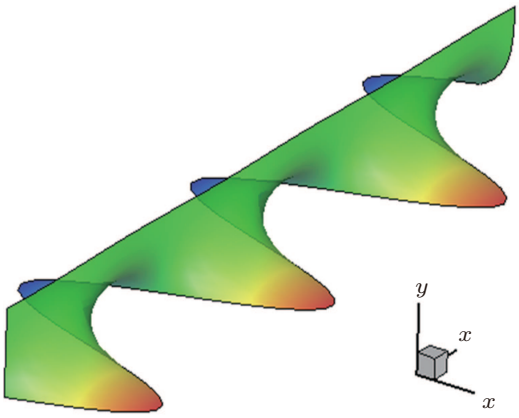


Fig. 3. (color online) Three-dimensional (3D) distribution of the spanwise Lorentz force in Eq. (4) at $k_x = 3$, $A = 1.0$, and $\Delta = 0.02$.

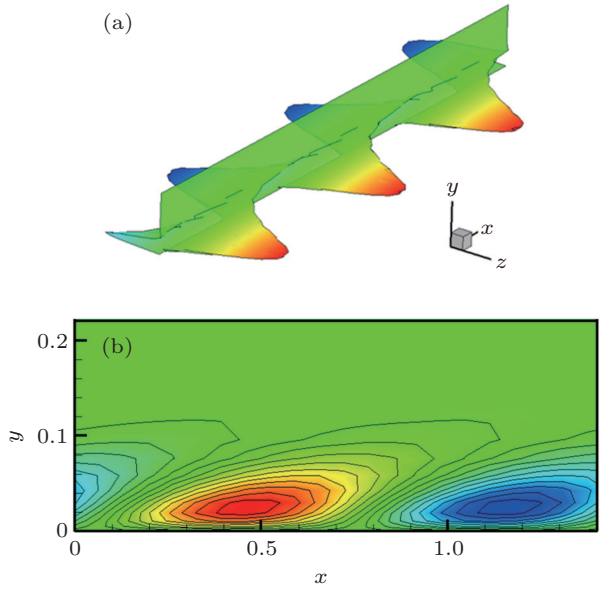
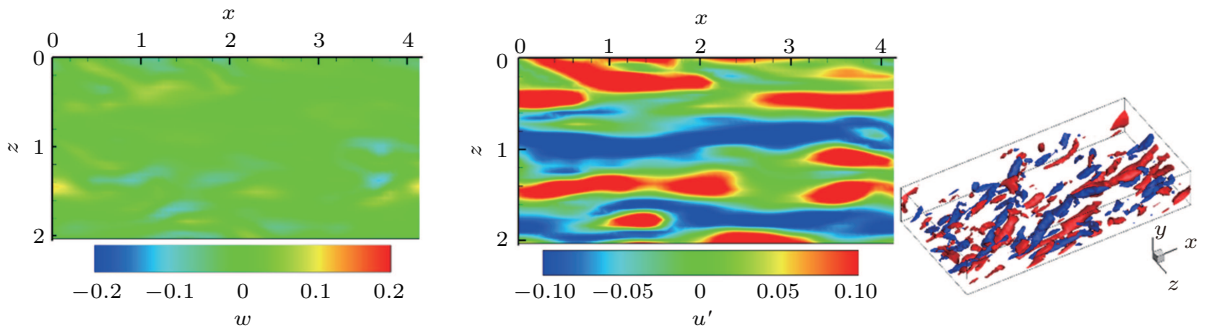


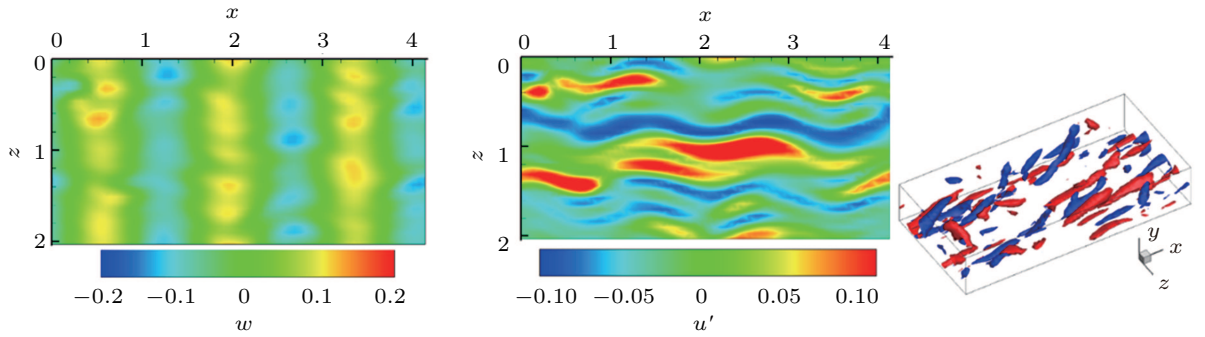
Fig. 4. (color online) Contours of the spanwise velocity induced by Lorentz force at $k_x = 3$, $A = 1.0$, and $\Delta = 0.02$ in the laminar flow for $Re = 4000$: (a) 3D distribution and (b) induced spanwise velocity shear layers in x–y plane.

3.2. Modulated flow fields

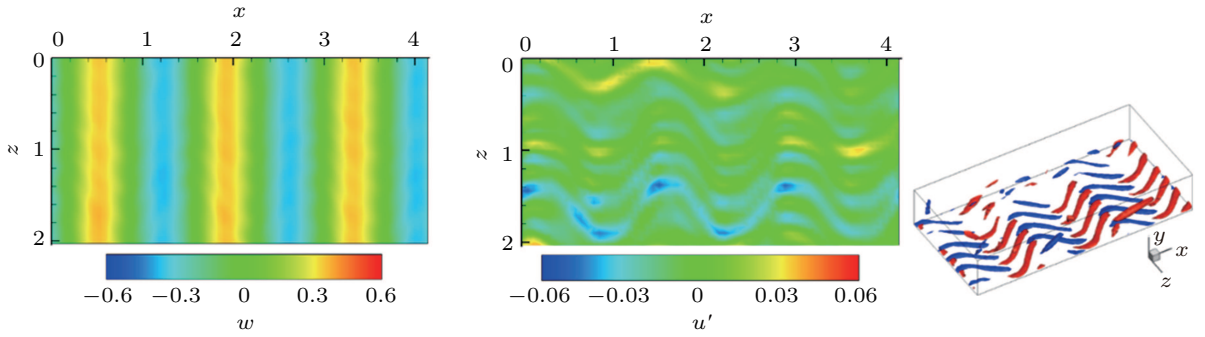
The streaks and the streamwise vortex structures are basic elements of the near-wall coherent structure of turbulence. The Lorentz force in Eq. (4) depends on amplitude A and wave number k_x, where A is the magnitude of the force, and k_x the streamwise distribution. Therefore, the forces at different parameters have different control effects. The steady near-wall flow fields controlled by the Lorentz force at $k_x = 3$ are shown in Fig. 5. The first column shows the distributions of spanwise velocities w at $y^+ = 5$, where red and blue areas represent positive values $(+w)$ and negative values $(-w)$, respectively. An irregular and low-amplitude distribution of w in the uncontrolled case at $A = 0.0$ is shown in Fig. 5(a), which reflects the random character of the turbulent flow. Next, in Figs. 5(b)–5(e), $+w$ and $-w$ of controlled cases alternate along the streamwise direction, of which the period is the same as that of the Lorentz force and the value increases with the increase of the Lorentz force. The regularity of the spanwise velocity distributions increases first at small amplitudes ($A < 1.0$), which indicates the enhanced influences of the induced flow on the intrinsic flow, and then decreases ($A > 1.0$) due to the enhancement of the random fluctuations. The optimal effect is obtained at $A = 1.0$ corresponding to the flow field dominated by the induced flow. The second column shows the distributions of streaky structures at $y^+ = 5$, where the red areas represent high-speed streaks (streamwise fluctuation velocity $u' > 0$), and blue areas refer to low-speed ($u' < 0$). The high-speed and low-speed streaks of the uncontrolled case alternate along the spanwise direction and have different lengths and curvature degrees, which reflects the essential characters of the near-wall coherent structure of turbulence. The sinusoidal



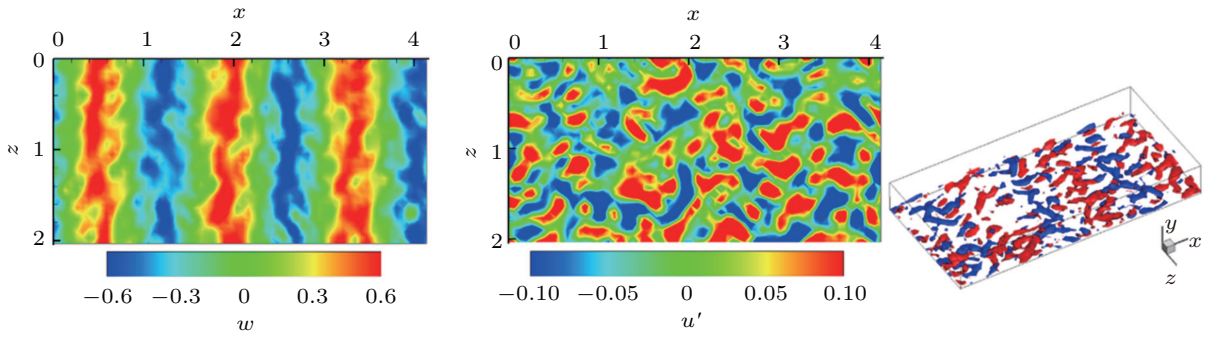
(a) $A = 0.0$



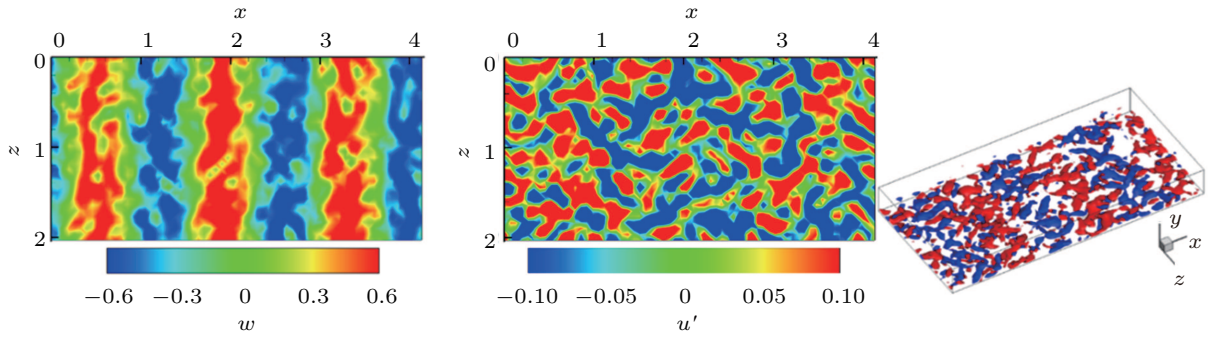
(b) $A = 0.3$



(c) $A = 1.0$



(d) $A = 2.0$



(e) $A = 3.0$

Fig. 5. (color online) Snapshots of spanwise velocity, streak, and vortex structure near the wall at $k_x = 3$, $\Delta = 0.02$, and different values of A.

distribution of streaks, of which the period is the same as that of the Lorentz force, is obtained in the controlled cases. With the increase of A, the intensity of streak first weakens ($A < 1.0$), then reaches the minimum at $A = 1.0$, and finally increases ($A > 1.0$). However, the regularity of streaks first increases ($A < 1.0$), then reaches the optimal condition at $A = 1.0$, and finally weakens gradually ($A > 1.0$) due to the enhancements of the irregular streaks. The third column shows the distributions of isosurfaces of vortex structures at $y+ = 0 - 100$, where red and blue areas represent positive and negative values of streamwise voticity, respectively. A large number of irregular quasi-streamwise vortices are obtained in an uncontrolled case. With the application of Lorentz force, the distributions of quasi-streamwise vortices have a significant improvement. The number and the intensities of the vortices first decrease ($A < 1.0$), then reach their minimum values at $A = 1.0$, where only a series of regular quasi-streamwise vortices are observed, and finally increase with the increase of A ($A > 1.0$).

The different control effects are obtained with the different values of wave number k_x, even with the same amplitude $A = 1.0$, which is shown in Fig. 6. Like the scenario in Fig. 5,

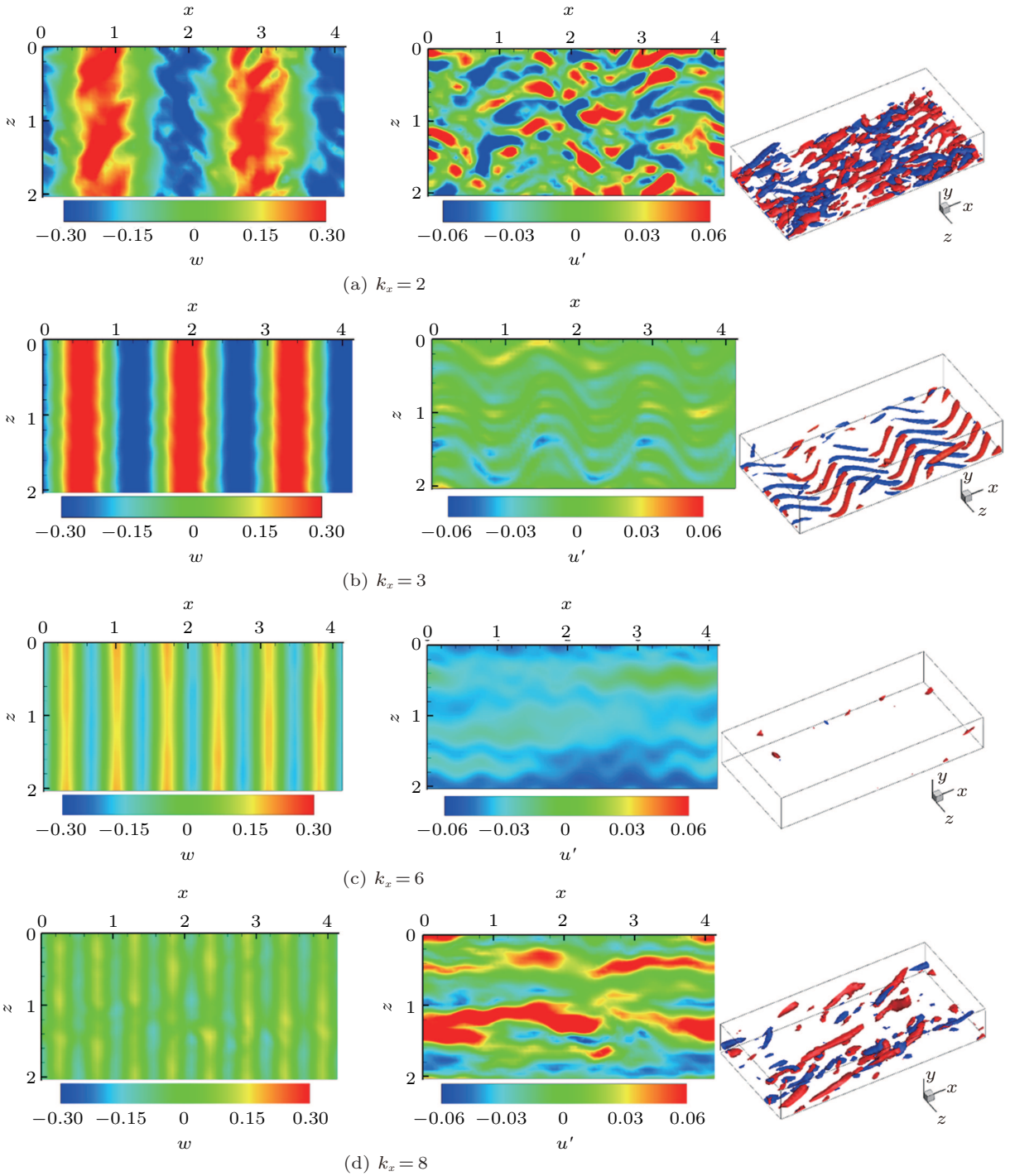


Fig. 6. (color online) Snapshots of spanwise velocity, streak, and vortex structure near the wall at $A = 1.0$, $\Delta = 0.02$, and different value of k_x.

the first, second and third column show the distributions of the spanwise velocities at $y^+ = 5$, the streaky structures at $y^+ = 5$ and the vortex structures at $y^+ = 0$–100 respectively, where the red and blue areas refer to corresponding positive and negative values, respectively. In the first column, the amplitude of w decreases with the increase of k_x, which indicates the decrease of spanwise motion induced by the Lorentz force. However, the regularity of w first increases, then reaches the optimal condition at $k_x = 3$, where the induced flow field dominates, and then weakens. With the increase of k_x in the second column, the intensity of the streak decreases and then increases, while the regularity of the distribution of the streaks increases and then weakens. The optimal control effect is the alternate distributions of the regular curve streaks along the spanwise direction at $k_x = 3$, of which the period is the same as that of the Lorentz force. In the third column, the number of the quasi-streamwise vortex structures first decreases and then increases with the increase of k_x. The number of the irregular vortices decreases dramatically at $k_x = 3$, and the rest of quasi-streamwise vortices have the periodical distributions along the streamwise with $+\omega_x$ and $-\omega_x$ alternating. Moreover, the regular vortex structures disappear and there are few vortex structures in the near-wall region at $k_x = 6$. Furthermore, the irregular vortices appear again at $k_x = 8$, which is similar to the flow field without control.

The variation of the flow fields leads to the variation of the Reynolds stress. The distributions of the mean Reynolds stress with the different parameters of Lorentz force are shown in Fig. 7, where figures 7(a) and 7(b) represent the variations of the mean Reynolds stress with A and k_x, respectively. The Lorentz force is exerted only near the lower wall at $y = -1$. The mean Reynolds stress first decreases then increases with the increase of A, especially in the near-wall region, and finally reaches a minimum at $A = 1.0$. The near-wall flow is modified by Lorentz force, of which the effect is enhanced with the increase of A as shown in Figs. 5(a)–5(c). The irregular quasi-streamwise vortices are eliminated, and the induced steady ones are generated in Fig. 5(c) at $A = 1.0$, which is corresponding to the minimum of the mean Reynolds stress. However, the random velocity fluctuations of turbulence are enhanced by overlarge amplitude A, which leads to a large number of irregular streaks and vortices as shown in Figs. 5(d)–5(e) and then enhances the mean Reynolds stress rapidly. The control effect of mean Reynolds stress first increases and then decreases with the increase of k_x in Fig. 7(b). The reason is that the near-wall flow is modified by Lorentz force, of which the effect first increases, then weakens with the increase of k_x as shown in Figs. 6(a)–6(d). Particularly, the mean Reynolds stress reaches the minimum at $k_x = 3$ due to the generation of steady structures of quasi-streamwise vortexes, which is induced by Lorentz force as shown in Fig. 6(b).

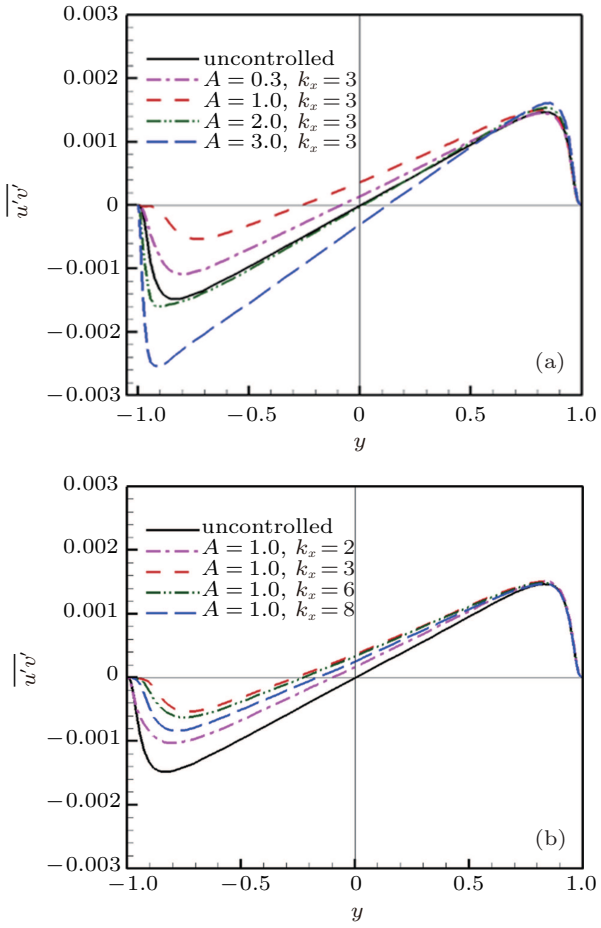


Fig. 7. (color online) Distributions of mean Reynolds stress $\overline{u'v'}$ with (a) $k_x = 3$, $\Delta = 0.02$, and different A, and (b) $A = 1.0$, $\Delta = 0.02$, and different values of k_x in a turbulent channel flow for $Re = 4000$.

Comparing the results at $k_x = 3$ and $k_x = 6$ from Figs. 6 and 7, the regular quasi-streamwise vortex structures are generated and small values of Reynolds stress are obtained at $k_x = 3$, which can be explained by the distributions of streamwise and wall-normal root mean square (rms) velocities, i.e., $u^+_{\rm rms}$ and $v^+_{\rm rms}$ in Fig. 8. Firstly, the control effects of $u^+_{\rm rms}$ and $v^+_{\rm rms}$ weaken with the increase of y^+ due to the decay of Lorentz force along the normal direction. Moreover, $u^+_{\rm rms}$ and $v^+_{\rm rms}$ decrease significantly in the near-wall region, because the induced spanwise motion has a suppression effect on the random velocity fluctuations. Then, the rms velocities in the two directions at $k_x = 3$ are both mostly smaller than those at $k_x = 6$, except $v^+_{\rm rms}$ in the near-wall region. However, the Reynolds stress is dominated by the variation of $u^+_{\rm rms}$. Therefore, the value of Reynolds stress at $k_x = 3$ is smaller than that at $k_x = 6$ in Fig. 7(b). It is indicated that the induced quasi-streamwise vortex structure has a further suppression effect on Reynolds stress.

The distributions of Lorentz force at $A = 1.0$ and $k_x = 3$ and the corresponding induced quasi-streamwise vortex structures are shown in Fig. 9, where red and blue colors refer to vortex structures with $+\omega_x$ and $-\omega_x$, respectively. The period of the vortex structures with alternate $+\omega_x$ and $-\omega_x$ is

the same as that of Lorentz force. Moreover, the vortex structures with $-\omega_x$ are generated by $+f_z$ and tilted into positive spanwise direction $+z$, and the ones with $+\omega_x$ are generated by $-f_z$ and tilted into negative spanwise direction $-z$.

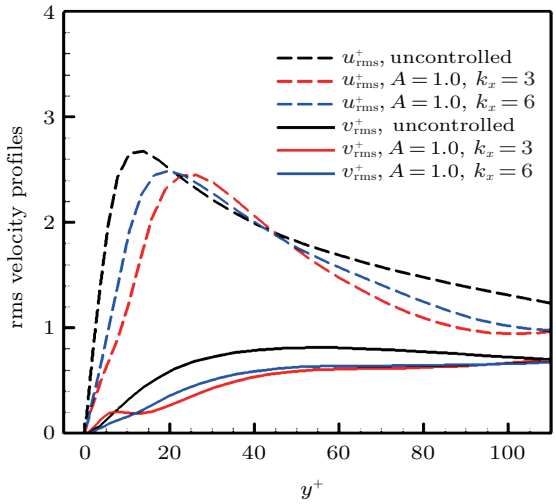


Fig. 8. (color online) Distributions of streamwise and wall-normal rms velocity without and with Lorentz force at $A = 1.0$, $\Delta = 0.02$, and $k_x = 3$ or $k_x = 6$ in turbulent channel flow for $Re = 4000$, respectively.

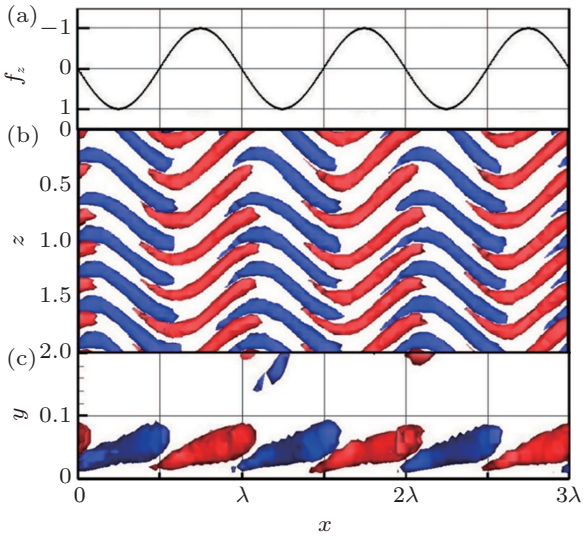


Fig. 9. (color online) Distributions of (a) Lorentz force in x–f_z plane and isosurfaces of induced vortex structures in (b) x–z plane and (c) x–y plane at $k_x = 3$, $A = 1.0$, and $\Delta = 0.02$ in a turbulent channel flow for $Re = 4000$.

As a case, a pair of the vortex structures with $+\omega_x$ and $-\omega_x$ is shown in Fig. 10. The vortex structure with $+\omega_x$ can be divided into three parts: the slightly curve tail on the left, induced by $-f_z$ and the upstream vortex with $-\omega_x$; the lifting and developing middle part, tilted by $-f_z$; and the head on the right reaching a top, then breaking down, meanwhile inducing a downstream vortex with $-\omega_x$. The vortex structure with $-\omega_x$ can be divided into three parts similarly.

Then, as shown in Fig. 11, the vortex structures with $-\omega_x$ are tilted into $+z$ by Lorentz force, and the ones with $+\omega_x$ are tilted into $-z$. However, these tilts of the two kind of vortex structures result in the spanwise vorticities in the same direction, i.e., negative spanwise vorticity $-\omega_z$.

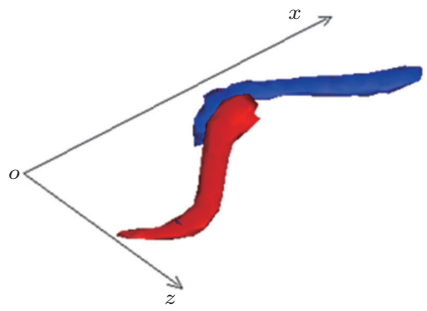


Fig. 10. (color online) Isosurface of a pair of vortex structures induced by Lorentz force at $k_x = 3$, $A = 1.0$, and $\Delta = 0.02$ in a turbulent channel flow for $Re = 4000$.

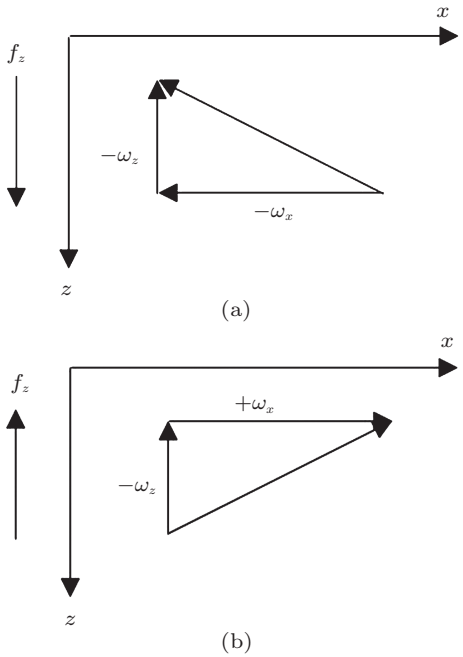


Fig. 11. Schematic diagram of directions of Lorentz force and vorticities of induced vortex structures at $k_x = 3$, $A = 1.0$, and $\Delta = 0.02$ in a turbulent channel flow for $Re = 4000$, showing negative spanwise vorticities induced by Lorentz force.

The effect of negative spanwise vorticity is shown in Fig. 12, and the velocity gradient can be reduced by the negative spanwise vorticity in the near-wall region of the turbulent boundary layer. Moreover, the location of the vorticity is consistent well with the model proposed by Choi and Clayton.[12]

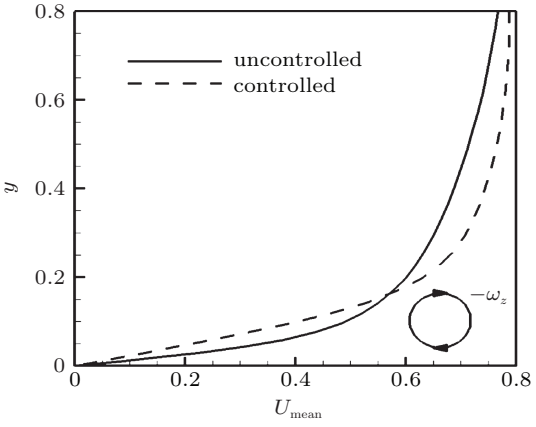


Fig. 12. Conceptual model for a turbulent channel flow controlled by Lorentz force, showing mean velocity profile affected by induced spanwise vorticity.

3.3. Control effects

The profiles of streamwise mean velocity with different control parameters are shown in Fig. 13, where figures 13(a) and 13(b) refer to the variations with A and k_x, respectively. From Fig. 13(a), the gradient of near-wall streamwise mean velocity first decreases and then increases with the increase of A, and finally reaches a minimum at $A = 1.0$. Similarly, from Fig. 13(b), this gradient also first decreases then increases with the increase of k_x, and reaches a minimum at $k_x = 3$. Moreover, the gradient of near-wall streamwise mean velocity at $k_x = 6$ is slightly larger than that at $k_x = 3$, due to a further improvement of the streamwise velocity gradient by the above mentioned negative spanwise voticity.

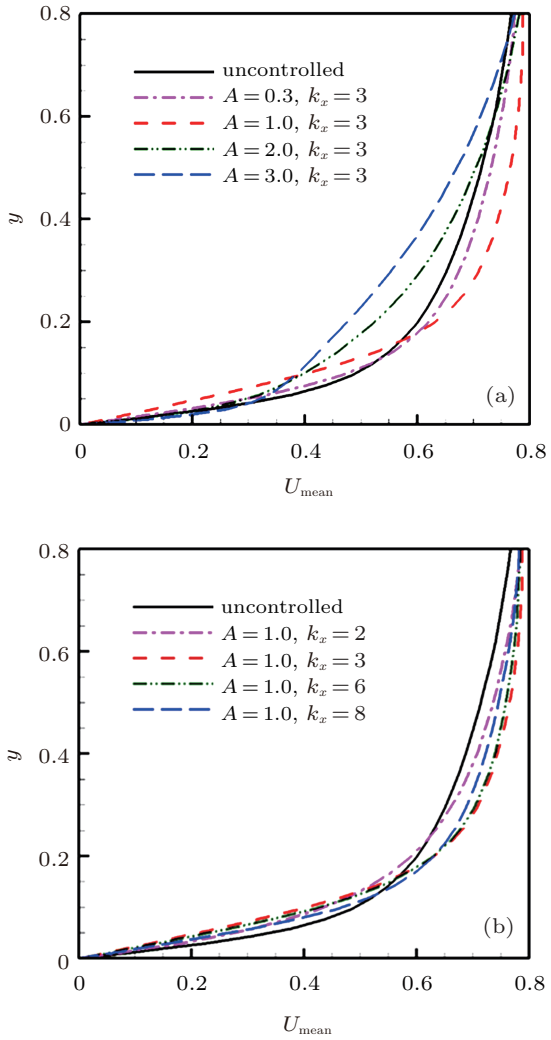


Fig. 13. (color online) Profiles of mean velocity with (a) $k_x = 3$, $\Delta = 0.02$, and different values of A and (b) $A = 1.0$, $\Delta = 0.02$ and different values of k_x in a turbulent channel flow for $Re = 4000$.

The drag reduction rate D_r, which is commonly used to measure the control effect, is simply given by[25]

$$D_r = (1 - \langle \tau_w \rangle / \langle \tau_{wn} \rangle) \times 100\%, \quad (5)$$

where $\langle \tau_w \rangle$ is the mean of wall shear stress with Lorentz force and $\langle \tau_{wn} \rangle$ without Lorentz force. The values of drag reduction rate D_r with the different parameters are shown in Fig. 14, where red areas refer to positive values of drag reduction rate and blue negative values, i.e., the increase of drag. From the figure, all the drag reduction rates first increase and then decrease with the increase of amplitude at different wave numbers. The D_r varies slowly at high wave numbers, and rapidly at low wave numbers with larger ranges of drag reduction and increase. Moreover, the above mentioned quasi-streamwise vortex structures at the parameters of $A = 1.0$ and $k_x = 3$ contribute to the decrease of random velocity fluctuation together with the reduction of Reynolds stress, and then improve the distributions of the streamwise velocity with the negative spanwise vorticities. Therefore, the optimal drag reduction of up to 58% can be obtained in this case.

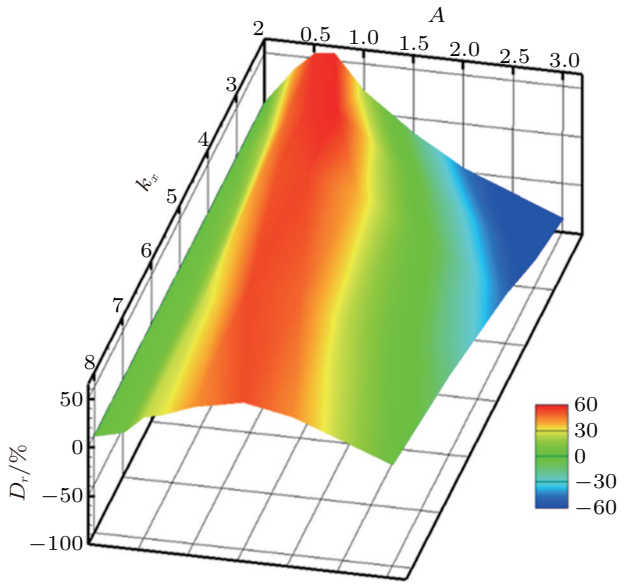


Fig. 14. (color online) Contour of drag reduction rate D_r with A and k_x of Lorentz force for $\Delta = 0.02$ and $Re = 4000$.

4. Conclusions

The control effects of the channel turbulent flow with the amplitude and the wave number of the spanwise Lorentz force are investigated with DNS based on Fourier–Chebyshev spectral method in this paper. The relations among the flow fields, mean Reynolds stress distributions, and drag reductions are discussed in depth. The results indicate that the Lorentz forces at different amplitudes and wave numbers have different control effects.The drag reduction rate first increases and then decreases both sharply with the increase of amplitude at low wave numbers while the variation of drag reduction rate at high wave numbers is similar to that at low wave numbers but slowly. The drag reductions of small values (or even drag increases) are due to the weak suppression or even the enhancements of the random velocity fluctuations and mean Reynolds stress. However, the efficient drag reduction is because of the regular quasi-streamwise vortex structure induced by Lorentz force, which contributes to suppressing the random velocity

fluctuation together with mean Reynolds stress, and the negative spanwise vorticity of the structure improves the distribution of streamwise velocity. Therefore, the optimal control effect with a drag reduction of up to 58% can be obtained.

References

[1] Song B W, Ren F, Hu H B and Huang Q G 2015 *Chin. Phys. B* **24** 014703
[2] Wang L, Xia Z X, Luo Z B, Zhou Y and Zhang Y 2014 *Acta Phys. Sin.* **63** 194702 (in Chinese)
[3] Cao Y F, Gu Y S, Cheng K M, Xiao Z Y, Chen Z B and He K F 2015 *Acta Aeronaut. Astronautics* **36** 757 (in Chinese)
[4] Zhang H, Fan B C and Chen Z H 2011 *Chin. Phys. Lett.* **28** 124701
[5] Zhang H, Fan B C, Chen Z H, Chen S and Li H Z 2013 *Chin. Phys. B* **22** 104701
[6] Li W, Jessen W, Roggenkamp D, Klaas M, Silex W, Schiek M and Schroder W 2015 *Eur. J. Mech. B: Fluids* **53** 101
[7] Boomsma A and Sotiropoulos F 2016 *Phys. Fluids* **28** 035106
[8] Bixler G D and Bhushan B 2013 *Adv. Funct. Mater.* **23** 4507
[9] Li Z X, Hu B P, Lan S L, Zhang J B and Huang J J 2015 *Computers & Fluids* **119** 26
[10] Touber E and Leschziner M A 2012 *J. Fluid Mech.* **693** 150
[11] Quadrio M 2011 *Phil. Trans. R. Soc. A* **369** 1428
[12] Choi K S and Clayton B R 2001 *Int. J. Heat Fluid Flow* **22** 1
[13] Whally R D and Choi K S 2014 *Exp. Fluids* **55** 1796
[14] Berger T W, Kim J, Lee C and Lim J 2000 *Phys. Fluids* **12** 631
[15] Lee J H and Sung H J 2005 *J. Turbul.* **6** 2
[16] Pang J, Choi K S, Aessopos A and Yoshida H 2004 *AIAA* 2004
[17] Pang J and Choi K S 2004 *Phys. Fluids* **16** 35
[18] Xu P, Choi K S and Jukes T 2006 *European drag reduction and flow control meeting*, 2006, Ischia, Italy
[19] Du Y Q and Karniadakis G E 2000 *Science* **288** 1230
[20] Du Y Q, Symeonidis V and Karniadakis G E 2002 *J. Fluid Mech.* **457** 1
[21] Xu P and Choi K S 2007 *Flow Control and MEMS* (Berlin: Springer) p. 259
[22] Quadrio M and Ricco P 2009 *J. Fluid Mech.* **627** 161
[23] Viotti C and Quadrio M 2009 *Phys. Fluids* **21** 105
[24] Yin J F, You Y X, Li W and Hu T Q 2014 *Acta Phys. Sin.* **63** 044701 (in Chinese)
[25] Huang L P, Fan B C and Dong G 2010 *Phys. Fluids* **22** 015103
[26] Huang L P, Choi K S, Fan B C and Chen Y H 2014 *Sci. China-Phys. Mech. Astron.* **57** 2133
[27] Wu W T, Hong Y J and Fan B C 2015 *Appl. Math. Mech.* **36** 1113
[28] Kim J, Moin P and Moser R 1987 *J. Fluid Mech.* **177** 133